J. Fluid Mech. (2008), *vol.* 599, *pp.* 299–307.
doi:10.1017/S0022112008000232 Printed in the United Kingdom

Closed-form solution of the potential flow in a contracted flume

G. BELAUD[1] AND X. LITRICO[2]

[1]UMR G-EAU, IRD, Maison des Sciences de l'Eau, 300 av. Emile Jeanbrau
34095 Montpellier Cedex 5, France
belaud@msem.univ-montp2.fr

[2]UMR G-EAU, Cemagref, B.P. 5095, 34196 Montpellier Cedex 5, France
xavier.litrico@cemagref.fr

(Received 23 October 2007 and in revised form 20 December 2007)

The potential flow upstream from a contraction in a rectangular flume is analysed. In order to calculate the potential function, the flow is considered as the superposition of sinks uniformly distributed in the contraction. The effect of boundaries is taken into account by introducing virtual sinks. The calculation is performed in the complex plane and provides a closed-form solution of the complex potential function. As an illustration, the effect of contraction size and position is analysed, and the solution is compared to experimental measurements and other numerical solutions for vertical sluice gates.

1. Introduction

The determination of the flow pattern in the vicinity of a sluice gate has many applications, such as the determination of the contraction coefficient, the calculation of the pressure force exerted on the gate or the determination of the distortion of the velocity profile induced by the contraction. Potential theory allows us to calculate explicitly the free streamlines past an orifice, and then the contraction coefficient (Batchelor 1967, § 6.13). Other studies have focused on the gravity effects for vertical or inclined gates (Benjamin 1956; Larock 1969; Chung 1972), and more recent studies have analysed, among other aspects, the effects on potential flow of the free-surface disturbances upstream from a gate (Montes 1997; Vanden-Broeck 1997; Binder & Vanden-Broeck 2007). Based on a comparison of his potential flow calculations with experimental data, Montes (1997) showed that the real fluid effects have little influence on the distribution of velocity and pressure. The determination of these functions is particularly useful to calculate the pressure exerted on the walls or to determine the velocity distribution for measuring purposes, for instance.

The potential flow problem is generally addressed by classical mapping of the physical plane and the complex potential plane. While the free-surface profile downstream from the gate can be determined explicitly in the case of non-gravity flow, the solutions developed by the investigators cited above, taking account of the presence of the free surface, require numerical schemes to evaluate the coordinates in the complex potential plane.

More generally, this problem can be extended to any rectangular channel where a contraction or an obstacle affects the streamlines. In this paper, we use the same assumption of irrotational and inviscid flow to derive a closed-form solution of the

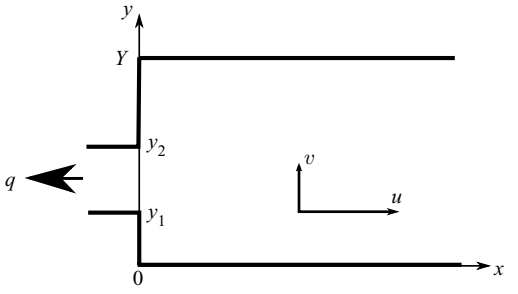

FIGURE 1. Sketch of the system studied.

potential flow upstream from such a rectangular contraction. Closed-form solutions may be particularly useful to validate or initialize numerical approaches, and the simplifying assumptions have proved to be sufficient in many engineering applications.

After deriving the expression for the potential function in the complex plane, we illustrate different configurations and compare them with experimental data and with numerical methods reported in the literature.

2. Potential flow solution

2.1. *Approach*

We consider the flow in a rectangular flume ended by a contraction. We perform a two-dimensional analysis of the flow upstream from the contraction, assuming that the flow is infinite in the third direction. The fluid is assumed to be homogeneous, inviscid and incompressible, and the flow to be irrotational. These assumptions allow us to apply the potential theory and the principle of superposition to obtain the flow field as a combination of elementary flows.

We use Cartesian coordinates with their origin at the flume contraction. The axes are denoted x and y (see figure 1 for the position and orientation of axes), while u and v represent the horizontal and vertical velocity components. The contraction edges are located at y_1 and y_2 respectively, and the flume limits are $y=0$ and $y=Y$. Discharge per unit width is denoted q, and mean velocity is defined as $U_0=q/Y$. Far from the contraction, the velocity magnitude is U_0 and velocity vectors are parallel to the flume boundaries. Next we search for the potential and stream functions upstream from the contraction, $\phi(x, y)$ and $\psi(x, y)$ respectively. We consider that the flow is generated by a distributed sink located at the contraction, the total discharge through the contraction being q. To perform the calculation, we first consider the contribution of an infinitesimal sink $\mathrm{d}q$, taking account of the flume boundaries. These boundaries are considered by superposing virtual sinks of the same strength, each boundary being a symmetry plane.

2.2. *Point sink solution in a bounded channel*

We consider an infinitesimal sink of discharge $\mathrm{d}q$, located at coordinates $(0, y_0)$. We use the complex coordinates, with $\mathrm{i}^2=-1$, $z=x+\mathrm{i}y$ (position or affix), $U=u-\mathrm{i}v$ (complex velocity), $F=\phi+\mathrm{i}\psi$ (complex potential) and $\mathrm{d}m=-\mathrm{d}q/\pi$ (sink strength). In z, the complex velocity generated by the sink in y_0, denoted $U^{(y_0)}(z)$, is

$$U^{(y_0)}(z)=\frac{\mathrm{d}m}{z-\mathrm{i}y_0}. \tag{2.1}$$

The complex potential function is obtained by integration of (2.1) with respect to z:

$$F^{(y_0)}(z) = \mathrm{d}m \log(z - \mathrm{i}y_0). \tag{2.2}$$

Impermeable boundaries are created at $y = 0$ and $y = Y$ by the addition of virtual sinks of the same strength. Each boundary must be a symmetry plane. If y_0 is the position of a sink on the vertical, we achieve symmetry by adding virtual sinks on the y-axis at $y = -y_0$, $y = 2Y - y_0$, $y = -2Y - y_0$, $y = 2Y + y_0$, $y = -2Y + y_0, \ldots,$ $y = 2nY - y_0$, $y = 2nY + y_0$, $y = -2nY - y_0$, $y = -2nY + y_0$, $n = 2, \ldots, \infty$. Therefore, the potential function, $F^{(y_0,b)}$, is obtained as follows:

$$F^{(y_0,b)}(z) = \sum_{n=-\infty}^{+\infty} \mathrm{d}m \log(z - (2nY - y_0)\mathrm{i}) + \sum_{n=-\infty}^{+\infty} \mathrm{d}m \log(z - (2nY + y_0)\mathrm{i}). \tag{2.3}$$

For the velocity field, we obtain

$$U^{(y_0,b)}(z) = \sum_{n=-\infty}^{+\infty} \frac{\mathrm{d}m}{z - (2nY - y_0)\mathrm{i}} + \sum_{n=-\infty}^{+\infty} \frac{\mathrm{d}m}{z - (2nY + y_0)\mathrm{i}}. \tag{2.4}$$

Closed-form expressions can be obtained using the following identity (Abramowitz & Stegun 1972, § 4.3):

$$\cot \xi = \frac{1}{\xi} + 2\xi \sum_{n=1}^{+\infty} \frac{1}{\xi^2 - n^2\pi^2} \tag{2.5}$$

where $\xi \mapsto \cot(\xi)$ denotes the cotangent function. Decomposing each term of the sum into fractions of $\xi - n\pi$ and $\xi + n\pi$, this identity can be rewritten as

$$\cot(\xi) = \sum_{n=-\infty}^{+\infty} \frac{1}{\xi + n\pi}; \tag{2.6}$$

then, with the change of variables $\xi' = \mathrm{i}\xi/a$, a and ξ being complex numbers different from 0:

$$\sum_{n=-\infty}^{+\infty} \frac{1}{\xi - \mathrm{i}n\pi a} = \frac{1}{a}\mathrm{i}\ \cot\left(\mathrm{i}\frac{\xi}{a}\right) = \frac{1}{a}\coth\left(\frac{\xi}{a}\right). \tag{2.7}$$

The complex velocity (2.4) is therefore equal to

$$U^{(y_0,b)}(z) = \frac{\mathrm{d}m\pi}{2Y}\left[\coth\left(\frac{\pi}{2Y}(z + \mathrm{i}y_0)\right) + \coth\left(\frac{\pi}{2Y}(z - \mathrm{i}y_0)\right)\right] \tag{2.8}$$

and the corresponding potential function is obtained by integration of (2.8) with respect to z:

$$F^{(y_0,b)}(z) = \mathrm{d}m\left[\log\left(\sinh\left(\frac{\pi}{2Y}(z + \mathrm{i}y_0)\right)\right) + \log\left(\sinh\left(\frac{\pi}{2Y}(z - \mathrm{i}y_0)\right)\right)\right]. \tag{2.9}$$

2.3. *Sink distribution in the contraction*

Experimental studies conducted on sluice gates (Finnie & Jeppson 1991; Roth & Hager 1999) suggest that the horizontal velocity component u can be considered as uniform at the contraction section ($x = 0$). These results were verified numerically by Montes (1997) for different contraction sizes. Such a configuration is obtained by considering a sink uniformly distributed between the points $(0,y_1)$ and $(0,y_2)$.

The principle of superposition allows us to derive the corresponding solution by integrating (2.4) and (2.9) with respect to y_0, between y_1 and y_2. The infinitesimal sink

strength is

$$\mathrm{d}m = -\frac{q}{\pi}\frac{\mathrm{d}y_0}{y_2 - y_1} \tag{2.10}$$

which yields the complex velocity:

$$U(z) = \mathrm{i}\frac{q}{\pi(y_2 - y_1)}\left[\log\left(\sinh\left(\pi\frac{z + y_2\mathrm{i}}{2Y}\right)\right) - \log\left(\sinh\left(\pi\frac{z + y_1\mathrm{i}}{2Y}\right)\right)\right] - \mathrm{i}\frac{q}{\pi(y_2 - y_1)}\left[\log\left(\sinh\left(\pi\frac{z - y_2\mathrm{i}}{2Y}\right)\right) - \log\left(\sinh\left(\pi\frac{z - y_1\mathrm{i}}{2Y}\right)\right)\right]. \tag{2.11}$$

To obtain the complex potential $F(z)$, the complex velocity U is now integrated with respect to z. Let us denote $g : \xi \mapsto g(\xi) = \log(\sinh(\xi))$ and G a primitive of g. Writing $g(\xi)$ as

$$g(\xi) = \log\left[\frac{\mathrm{e}^{\xi}}{2}(1 - \mathrm{e}^{-2\xi})\right] \tag{2.12}$$

$$= -\log(2) + \xi + \log(1 - \mathrm{e}^{-2\xi}) \tag{2.13}$$

we find a primitive G of g defined by

$$G(\xi) = -\xi\log(2) + \frac{\xi^2}{2} + \frac{1}{2}\mathrm{Li}_2(\mathrm{e}^{-2\xi}) \tag{2.14}$$

where $\mathrm{Li}_2(\xi)$ denotes the dilogarithm of ξ (Abramowitz & Stegun 1972, § 27.7), defined as the primitive of $\xi \mapsto -\log(1 - \xi)/\xi$ being null in 0. When $|\xi| < 1$, $\mathrm{Li}_2(\xi)$ is also equal to

$$\mathrm{Li}_2(\xi) = \sum_{n=1}^{\infty}\frac{\xi^2}{n^2} \tag{2.15}$$

In the domain $\mathrm{Re}(\xi) > 0$, we have $|\mathrm{e}^{-2\xi}| < 1$ and (2.15) provides a method to compute the dilogarithm. An excellent approximation of the complex dilogarithm is also given by Clamond (2006).

After a few simplifications, the potential function is given by

$$F(z) = -\frac{q}{Y}z + \frac{q\log 2}{\mathrm{i}\pi} + \frac{2qY\mathrm{i}}{\pi^2(y_2 - y_1)}\left(L\left(\frac{z + y_2\mathrm{i}}{Y}\right) - L\left(\frac{z + y_1\mathrm{i}}{Y}\right) - L\left(\frac{z - y_2\mathrm{i}}{Y}\right) + L\left(\frac{z - y_1\mathrm{i}}{Y}\right)\right) \tag{2.16}$$

where

$$L(\xi) = \tfrac{1}{2}\mathrm{Li}_2(\mathrm{e}^{-\pi\,\xi}). \tag{2.17}$$

Equation (2.16) is the exact solution of the potential flow generated by the distributed sink in the rectangular channel. Note that the second term of the complex potential function, $q\log 2/\mathrm{i}\pi$, is constant and can therefore be omitted. Far from the contraction, $\mathrm{Re}(z/Y) \to +\infty$ and $\mathrm{e}^{-\pi\mathrm{Re}(z)/Y} \to 0$. Since $\mathrm{Li}_2(0) = 0$, the complex potential function can be approximated by

$$F(z) \approx -U_0\, z \tag{2.18}$$

which is the potential function for a uniform velocity field. Finally, we obtain the potential and stream functions $\phi(x, y)$ and $\psi(x, y)$ defined as the real and imaginary parts of $F(x + \mathrm{i}y)$.

To refine the flow analysis near the contraction, we may choose different sink distributions, taking into account some heterogeneity of the horizontal velocity in the contraction section. The same framework can be applied, but we have no guarantee of obtaining a closed-form solution for U and F. In this case, integration of (2.8) and (2.9) must be performed numerically. We show in the next section that the uniform distribution gives an accurate description of the velocity and pressure fields upstream from the contraction.

3. Some illustrations and applications

The derived equations apply to any set of values $0 \leqslant y_1 < y_2 \leqslant Y$. To illustrate the interest of the approach, we first calculate the iso-potential and streamlines for different configurations in order to analyse the effects of the boundaries and of the sink distribution on the flow field. Then, we focus on the configuration of the vertical sluice gate and compare our solution to experimental data and numerical results provided by different authors. To simplify the notation, we denote $W = y_2 - y_1$ (contraction breadth) and $Y_0 = (y_1 + y_2)/2$ the position of the contraction centre.

3.1. *Potential and streamlines*

In this section, we consider $Y = 1\,\mathrm{m}$ and a unit discharge $q = 1\,\mathrm{m^2\,s^{-1}}$. We plot different figures to illustrate the effects of boundaries and of the contraction size on the flow field. Figure 2(*a*) presents the solution plotted using (2.16) for a centred contraction ($Y_0 = Y/2$) with an opening $W = Y/10$. In the close vicinity of the orifice (figure 2*b*), the iso-potential lines deviate significantly from the point sink solution (which yields circles centred around the sink). The present solution, which gives a finite potential, is more realistic, as already shown by Shammaa, Zhu & Rajaratnam (2005) with a numerical approach. At a larger distance from the orifice, the distortion of the iso-potential lines is due to the presence of boundaries. This effect is more visible in the case of an orifice close to the boundary ($Y_0 = 0.25Y$, figure 2*c*). The effect of the contraction size can be observed by comparing figure 2(*a*) ($W = Y/10$) with figure 2(*d*) ($W = Y/2$).

3.2. *Velocity profile*

In the next two sections, the configuration represents a vertical sluice gate, one boundary of the contraction being the bottom. The y-axis is vertical and oriented upward. Taking $y_1 = 0$, (2.11) simplifies to

$$U(z) = \mathrm{i}\frac{q}{\pi W}\left[\log\left(\sinh\left(\pi\frac{z + y_2\mathrm{i}}{2Y}\right)\right) - \log\left(\sinh\left(\pi\frac{z - y_2\mathrm{i}}{2Y}\right)\right)\right]. \qquad (3.1)$$

A practical application is the velocity profile distortion on approaching the contraction. This phenomenon has been studied experimentally by Roth & Hager (1999) and Rajaratnam & Humphries (1982). In these papers, the distortion was presented by plotting the horizontal velocity component as a function of the vertical axis y, at different distances x from the contraction. With our approach, the horizontal component $u(x, y)$ is obtained by taking the real part of $U(x + \mathrm{i}y)$.

Figure 3 compares the present solution with the data provided by Rajaratnam & Humphries (1982), experiment B1. The flow data are: $Y = 0.42\,\mathrm{m}$, $Y_0 = W/2 = 0.025\,\mathrm{m}$, $q = 0.0843\,\mathrm{m^2\,s^{-1}}$, and they measured the velocity components at 0.1 m, 0.5 m and 1 m upstream from the orifice. The comparison is shown on figure 3(*a*). The correspondence between the model and the data is good, except in the close vicinity of

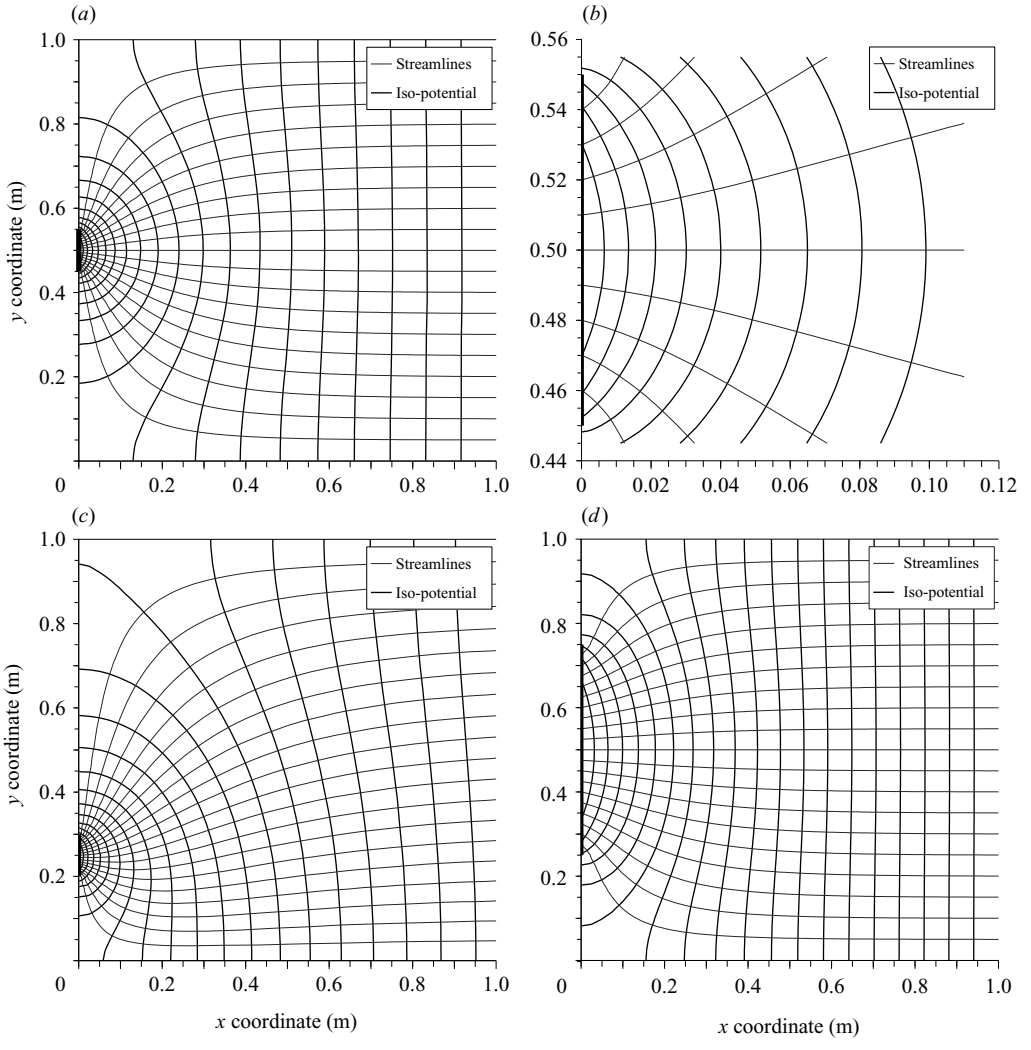

FIGURE 2. Iso-potential and stream lines: (*a*) $Y_0 = Y/2$, $W = Y/10$ and (*b*) a close-up near the orifice; (*c*) $Y_0 = Y/4$, $W = Y/10$; (*d*) $Y_0 = Y/2$, $W = Y/2$.

the boundaries. The corresponding velocity field and the iso-velocity lines are shown in figure 3(*b*).

3.3. *Pressure field*

The pressure field exerted on vertical gates has been studied experimentally by several authors (Rajaratnam & Humphries 1982; Roth & Hager 1999) and numerically by Montes (1997). Using the present velocity calculation, we apply the principle of energy conservation along the vertical streamline on the upstream face of the gate. We obtain the pressure at elevation y on the upstream face of the gate:

$$p(y) = \rho g(H - y) - \tfrac{1}{2}\rho v^2(y) + p_0 \tag{3.2}$$

where $v(y)$ is the vertical component of the velocity on the upstream face of the gate, H is the water height upstream from the gate, g is the acceleration due to gravity, ρ the specific weight of the fluid and p_0 the atmospheric pressure (constant). For

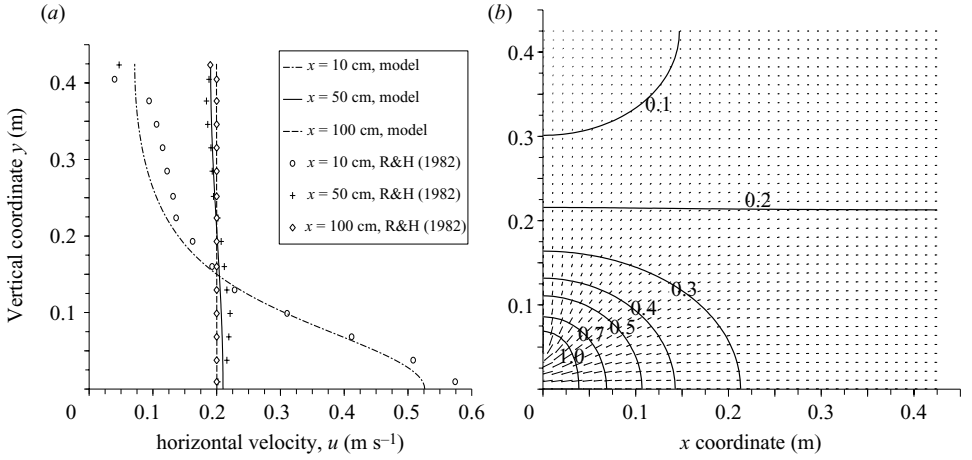

FIGURE 3. Comparison of our calculation with measurements by Rajaratnam & Humphries (1982) (exp. B1): (*a*) horizontal velocity $|u|$ at $x = 0.1$ m, 0.5 m and 1 m (x is the distance from the gate); (*b*) iso-kinetic lines and velocity vectors.

simplicity, we take $p_0 = 0$, p being the gauge pressure. The velocity component is calculated using (2.11):

$$v(y) = -\frac{q}{\pi W} \log\left(\frac{\sin(\pi(y+y_2)/2H)\sin(\pi(y-y_1)/2H)}{\sin(\pi(y-y_2)/2H)\sin(\pi(y+y_1)/2H)}\right) \tag{3.3}$$

where y_2 denotes the upper limit of the orifice under the gate, y_1 the lower limit of the orifice. Note that this equation applies to a vertical gate above a sharp-crested weir. In the case of a gate on a flat bed, $y_2 = W$ and $y_1 = 0$. Equation (3.3) simplifies to

$$v(y) = -\frac{q}{\pi W} \log\left(\frac{\sin \pi(y+W)/2H}{\sin \pi(y-W)/2H}\right) \tag{3.4}$$

and

$$p(y) = \rho g(H-y) - \frac{1}{2}\frac{\rho U_0^2}{\pi^2}\left(\frac{H}{W}\right)^2 \log^2\left(\frac{\sin \pi(y+W)/2H}{\sin \pi(y-W)/2H}\right). \tag{3.5}$$

Figure 4 compares the present calculation with the numerical calculation of Montes (1997) for $H/W = 3$ in free flow conditions. There is very little difference in the results. The model also fits very well the large data set provided by Roth & Hager (1999). However, the edge ($x = 0$, $y = W$) is a singular point and the vertical velocity v has an infinite magnitude. This causes the relative pressure p to be negative, whereas it should be equal to 0 since this point is the start of the free streamline under the gate.

The limit value of y where $p(y) \geqslant 0$, denoted y_l, can be obtained by solving $p(y_l) = 0$ numerically. Since y_l is close to W, a development in Taylor series gives a good approximation of y_l:

$$y_l \simeq W + \frac{2H}{\pi}\frac{\alpha}{1-\alpha\beta} \tag{3.6}$$

with

$$\alpha = \sin\left(\frac{\pi W}{H}\right)\exp\left[-\frac{\pi W}{U_0 H}\sqrt{2g(H-W)}\right] \quad \text{and} \quad \beta = \cot\left(\frac{\pi W}{H}\right) + \frac{W}{U_0}\sqrt{\frac{2g}{H-W}}.$$

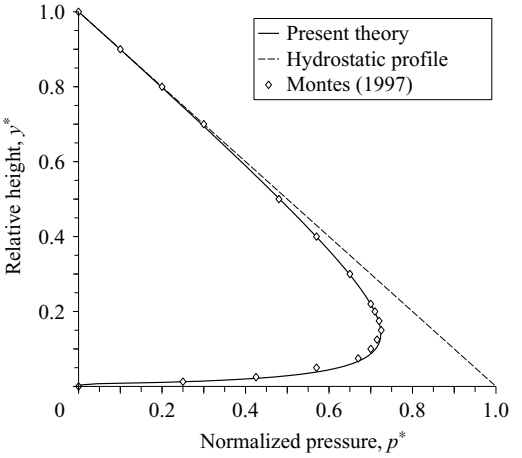

FIGURE 4. Comparison of the pressure profiles predicted by Montes (1997) for a vertical gate in free flow, $H/W = 3$, and our calculation. Pressures are relative to atmospheric pressure ($p_0 = 0$). The normalized pressure is defined by $p^*(y^*) = p(y)/\rho g(H - W)$ and the relative position is $y^* = (y - W)/(H - W)$.

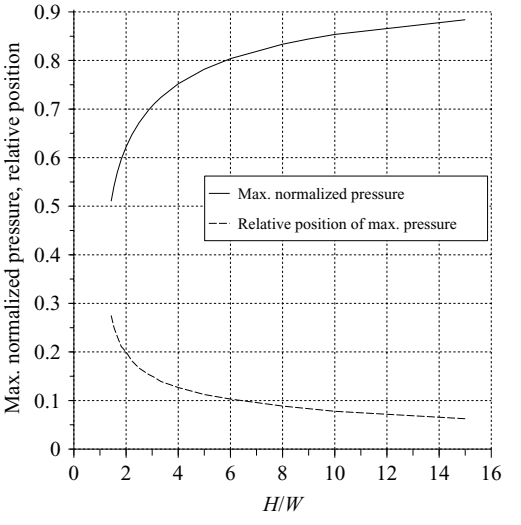

FIGURE 5. Maximum value of normalized pressure $P^* = \max(p(y)/\rho g(H - W)$ and relative position of the maximum pressure.

For the example presented in figure 4, the exact value of y_l is given by $(y_l - W)/(H - W) \approx 0.0084$, which is the value obtained with the approximate method (3.6) with a relative error of 5×10^{-6}.

The position and the value of the maximum pressure are easy to determine, for example by solving the equation $p'(y) = 0$. The results (figure 5) are very close to those presented by Montes (1997) validated with experimental data. We can conclude that the present solution gives an accurate description of the pressure force on the gate, although it cannot be used to predict the local pressure at the contraction edge, which is a singular point.

4. Conclusion

We derived a closed-form solution of the potential flow upstream from a contraction in a rectangular flume. The main assumptions are that the flow is irrotational and inviscid, and the contraction is taken into account by a homogeneous sink distribution. With these assumptions, we obtain the exact solution of the potential flow, and no approximation is required. Unlike previous calculations, the problem is solved directly in the physical plane, and does not require conformal transformation between the physical plane and the complex potential plane.

Since the complex function and the velocity components are expressed explicitly, computation is very quick. The derived solution can be applied to asymmetric configurations, such as vertical sluice gates on a flat bed. The calculated velocity and pressure fields are in very good agreement with previous computations and experiments. One possible application is the calculation of the pressure force on a vertical sluice gate. The present solution can also be used for other configurations using conformal transformations.

REFERENCES

Abramowitz, M. & Stegun, I. A. 1972 *Handbook of Mathematical Functions*. US Department of Commerce.

Batchelor, G. K. 1967 *An Introduction to Fluid Dynamics*. Cambridge University Press.

Benjamin, T. B. 1956 On the flow in channels when rigid obstacles are placed in the stream. *J. Fluid Mech.* **1**, 227–248.

Binder, B. J. & Vanden-Broeck, J. M. 2007 The effect of disturbances on the flows under a sluice gate and past an inclined plate. *J. Fluid Mech.* **576**, 475–490.

Chung, Y. K. 1972 Solution of flow under sluice gates. *ASCE J. Engng Mech. Div.* **98**, 121–140.

Clamond, D. 2006 Complex dilogarithm. *Tech. Rep.* Available from Matlab exchange central, http://www.mathworks.com.

Finnie, J. & Jeppson, W. 1991 Solving turbulent flows using finite elements. *J. Hydraul. Engng* **117**, 1513–1530.

Larock, B. 1969 Gravity-affected flow sluice gate. *ASCE J. Hyd. Div.* **95**, 153–176.

Montes, J. S. 1997 Irrotational flow and real fluid effects under planar sluice gates. *J. Hydraul. Engng* **123**, 219–232.

Rajaratnam, N. & Humphries, J. A. 1982 Free flow upstream of vertical sluice gates. *J. Hydraul. Res.* **20**, 427–437.

Roth, A. & Hager, W. 1999 Underflow of standard sluice gate. *Exps. Fluids* **27**, 339–350.

Shammaa, Y., Zhu, D. Z. & Rajaratnam, N. 2005 Flow upstream of orifices and sluice gates. *J. Hydraul. Engng* **131**, 127–133.

Vanden-Broeck, J. M. 1997 Numerical calculations of the free-surface flow under a sluice gate. *J. Fluid Mech.* **130**, 339–347.